

EXPERIMENTAL EVALUATION OF THE VELOCITY PROFILES AND PERFORMANCE OF A COUNTER ROTATING MICRO-TURBINE BY 2D LASER DOPPLER VELOCIMETRY

Elena VAGNONI*

École polytechnique fédérale de Lausanne, Laboratory for Hydraulic Machines, Lausanne, Switzerland

Loïc ANDOLFATTO

École polytechnique fédérale de Lausanne, Laboratory for Hydraulic Machines, Lausanne, Switzerland

Cécile MÜNCH-ALLIGNÉ

HES SO Valais, Haute école spécialisée de Suisse occidentale, Sion, Switzerland

François AVELLAN

École polytechnique fédérale de Lausanne, Laboratory for Hydraulic Machines, Lausanne, Switzerland

ABSTRACT

The most exploited renewable energy at a global scale is hydropower, which nowadays accounts for the 18 % of the world's electricity supply. Its production is expected to increase approximately 3.1% each year in the next 25 years maintaining its share in the mix of electricity sources. Concerning small scale hydropower, some of the current research is focusing on the limitation of the environmental impact and economical investments. The development of energy recovery systems on existing water utility networks is a new challenge for increasing the sustainability of hydroelectricity generation. The concept of the new counter rotating micro-turbine braces this goal by allowing the recovery of the energy which is spoiled in pressure reducing valves in the water supply network. The performance of the micro-turbine prototype has been evaluated through experimental campaigns involving pressure, torque, discharge measurements and 2D Laser Doppler Velocimetry (LDV). A dedicated transparent casing equipped with flat windows has been built in order to perform undistorted optical measurement and to limit the refraction and reflection of the laser beam. The velocity profiles of the axial and tangential components have been measured for several radial positions at the inlet, in the gap between the two runners and at the outlet section of the micro-turbine prototype. Numerical simulations and a further study on the mass equation applied to the investigated cross-sections of the machine have been carried out in order to complete the velocity profile where the optical access to perform LDV measurements had been blocked. These experimental methods grant a full study on the velocity profiles. The energy equation, applied to the outlet sections of both runners, allows the investigation of the flow behavior and of the related machine performance. The results back up further improvements of the runner blades shape.

KEYWORDS

Small hydropower, axial micro-turbine, counter rotating runners, LDV.

* *Corresponding author:* EPFL STI LMH, Avenue du Cour 33 bis, Lausanne, Switzerland, phone:
+41 21 693 36 43, elena.vagnoni@epfl.ch

1. INTRODUCTION

Small scale hydropower, defined as the hydropower production up to 10MW, has been drawing increasing attention in the past years for the development of new competitive technologies in the field of renewable energies. In Switzerland its production accounts for the 5.7 % of the electricity mix and it is expected to increase by 50 % in 2050.

In order to achieve competitive performances in the market of renewable energy sources, small scale hydropower is required to maintain low investments and a low environmental impact [1]. The counter rotating micro-turbine satisfies these requirements. Recovery systems in existing infrastructures are a new concept of technology to recover the energy lost by pressure reducing valve in water supply networks. Computational Fluid Dynamics (CFD) studies have been carried [2] to assess the hydraulic performance and the flow velocity fields of the turbine. A physical model of the designed runners of the counter rotating micro-turbine has been built to perform experimental investigations for having a complementary study on both the hydraulic performance and the flow velocity fields. Pressure, torque and discharge measurements combined with Laser Doppler Velocimetry (LDV) investigations have been carried out to explore both the performance and the full velocity profiles in the counter rotating micro-turbine [3] [4].

Non-intrusive optical measurements such as LDV are experimental techniques prominently developed in the past few years. These techniques fit well turbomachinery applications as past studies such Gagnon *et al.* [5] proved. On the other hand, as investigated by Zaidi *et al.* [6], precise results by these laser and optical measurement techniques are often difficult to achieve since parameters such refraction index of both the material interface and the flow, laser alignment, seeding and machine geometry are fundamental to obtain successful results.

Cunning set-up have been developed in the past, Müller *et al.* [7] used water boxes to mitigate the effects of optical distortion for laser measurements and flow visualizations. There exist examples of complete optical access through the blades of a turbomachine. Uzol *et al.* [8] constructed an index-matched facility, in which the refractive index of the fluid is matched with that of transparent blades. Miorini *et al* [9] used the same approach to examine flow in the tip region of a waterjet pump.

A resolved arrangement to achieve precise optical measurements in different positions in the counter rotating micro-turbine although the harsh geometry and size of the machine has been designed. Nevertheless the full flow velocity profiles couldn't be achieved close to the hub due to the high reflection of the laser beam on the hub wall. Thus in order to fulfill the velocity profiles in the region where LDV measurements were not achieved, a study on the mass balance equation has been performed along with the prediction of the flow velocity fields obtained by the numerical simulations. Moreover a method based on the resolution of the total specific rothalpy balance equation has been employed to compute the transferred power of the micro-turbine and to compute the efficiency.

2. EXPERIMENTAL SET-UP

2.1. TEST FACILITY

The runner counter rotating micro-turbine is a single stage axial turbine with two counter rotating runners. The first runner features 5 blades and the second runner 7 blades, respectively; the relevant geometrical parameters are summarized in Tab.1. The micro-turbine has been installed in an elbow pipe in the test facility illustrated in Fig.1.

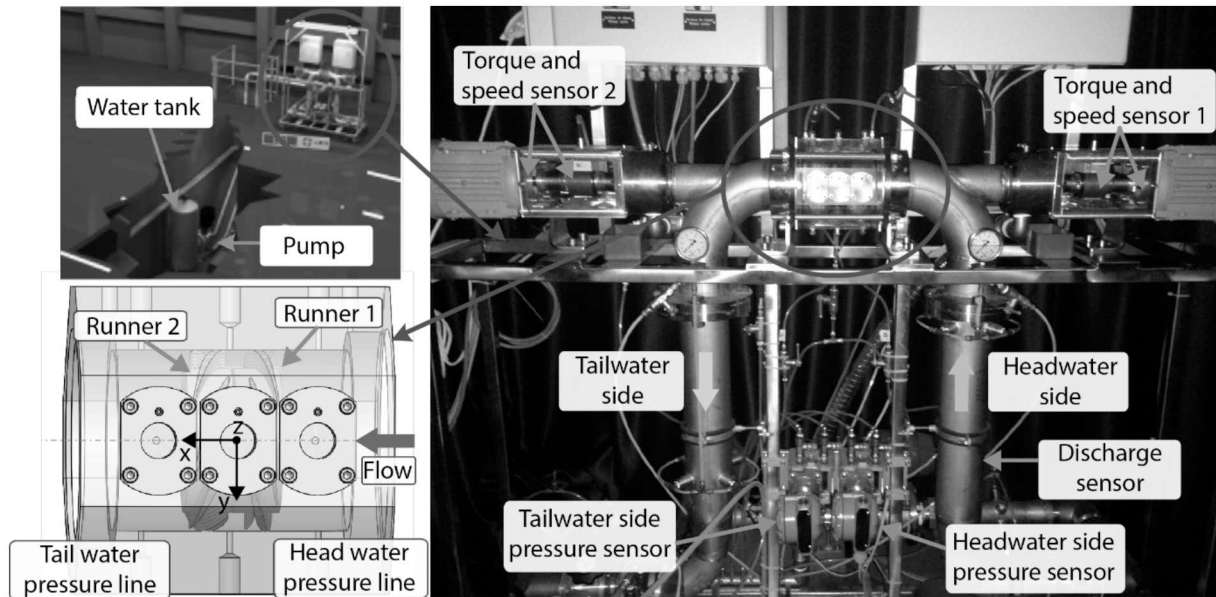


Fig.1 Side view of the test facility.

The elbow has been designed for having an axial flow at the turbine inlet. A honeycomb is located upstream the inlet section in order to minimize the non-uniformities and large scale turbulence at the inlet of the first runner. An external pump feeds the facility taking water from an atmospheric pressure water tank and is controlling the head for different machine operations. The facility is equipped with two differential pressure transducers measuring the difference of the static pressure between the headwater and the tailwater sections as shown in Fig.1. The 2 sections being of the same area, this measurement yields the specific energy E according to Eq.(1).

$$E_h = \frac{p_t - p_{\bar{t}}}{\rho} = \frac{\Delta p}{\rho} \quad (1)$$

An electromagnetic flowmeter located upstream the machine measures the discharge and this value is corrected by a loss coefficient due to the leakages through the seals. Each runner shaft is equipped with a strain gauges torquemeter for measuring the runner torque.

The runners are installed in a transparent casing. As illustrated in Fig.1 the casing has been equipped with three optical circular windows made of N-BK7 glass. The thickness of the glass windows is 6 mm with a 32.5 nm flatness. This has been designed in order to obtain a casing segment which avoids distortion of the laser beam and enlargement of the control volume during LDV measurements.

The operating conditions and performance of the micro-turbine have been predicted by Münch-Alligné *et al.* [2]. Steady numerical simulations have been performed by using the Unsteady Reynolds Average Navier-Stokes (URANS) code with the commercial software ANSYS CFX 13.0. The operation conditions for the predicted design point are resumed in Tab.1. Experimental investigations have been also performed and allowed to build the hillchart of the machine as presented by Andolfatto *et al.* [3].

PARAMETERS	SYMBOL	VALUE
INNER CASING AND OUTFLOW SECTION DIAMETER	D_1	100 mm
SHROUD RADIUS	R_s	50 mm
HUB RADIUS	R_h	40 mm
TIP PROFILE CHORD LENGTH	c	60 mm
TIP PROFILE AXIAL CHORD LENGTH	c_a	20.67 mm
TIP CLEARANCE	s	0.1 mm
RUNNERS SPEED DESIGN POINT	N_1, N_2	3000 min ⁻¹
SPECIFIC ENERGY DESIGN POINT	E	196 J kg ⁻¹
DISCHARGE DESIGN POINT	Q	8.5 10 ⁻³ m ³ s ⁻¹
EFFICIENCY DESIGN POINT	η	0.85

Tab.1 Runners geometry and design point operation conditions.

2.2. LASER DOPPLER VELOCIMETRY

The LDV system is a Dantec FlowExplorer compact LDA with 2 laser beams at 660 and 775 nm. It is composed of a 300 mW solid state laser source, a beam splitter and an optical probes of 300 mm focal length. The seeding particles are 10 μ m diameter hollow glass spheres with a density that is almost the same as the one of water. It is therefore assumed that the particles perfectly behave as the liquid flow. A remotely controlled traversing system is used for the radial displacement of the laser. LDV measurements have been performed to measure the average meridional component (along the x direction) and the tangential component (along the y direction) of the absolute flow velocity at different positions across the two runners. The origin of the Cartesian coordinate system is located between the two runners on the axis of the machine as shown in Fig.2. The point for which the location is controlled during the measurement is the center of the measurement volume. The measurements have been performed at 3 positions along the x axis, as indicated in Fig 2: at the inlet of the first runner (Inlet section), between the two runners (Inter-runners section) and at the outlet of the machine (Outlet section). For each axial position, 8 locations on the z axis have been investigated with 1 mm spatial resolution. Further radial positions closer to the hub couldn't be investigated because of the intense reflection of the laser beams on the hub wall. For each location at each reference point 20000 samples have been recorded and the maximum measurement duration has been set to 30 s. Fig.2 schematizes the chain of acquisition.

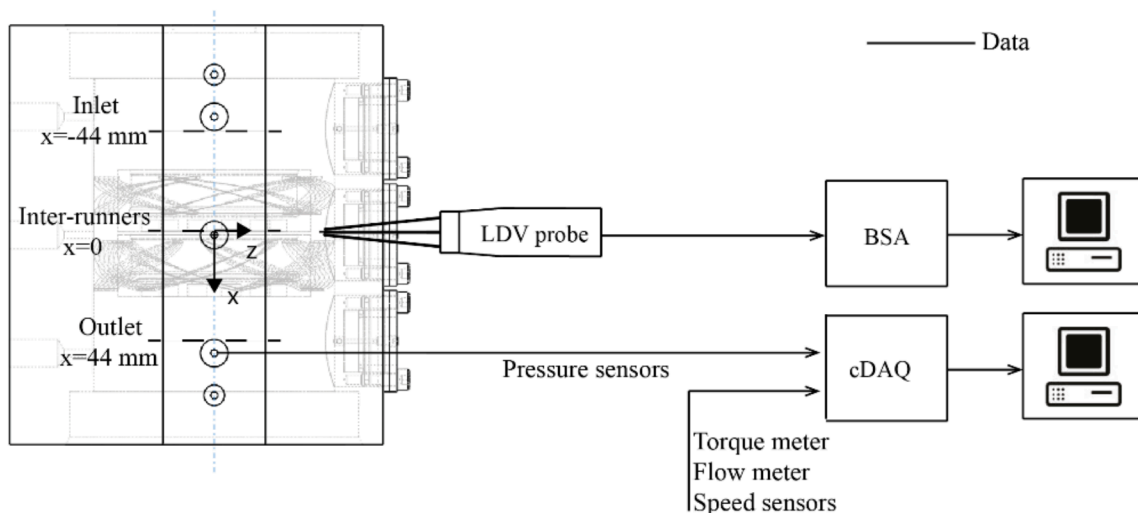


Fig.2 Top view of the micro-turbine runners with the LDV experimental set-up.

2.3. EXPERIMENTAL CONDITIONS

Measurements have been performed at several operation conditions which reach the highest efficiency for selected discharges based on the results obtained by previous measurements [3]. All the investigated operation conditions keep a relative rotational speed coefficient $\alpha = \left| \frac{\omega_1}{\omega_2} \right| = 1$. The operation parameters are resumed in Tab.2.

Test	DISCHARGE [m ³ s ⁻¹]	ENERGY [J kg ⁻¹]	RUNNERS ROTATIONAL SPEED [min ⁻¹]	MEASURED EFFICIENCY [%]	COMPUTED EFFICIENCY [%]
TEST A	6.3 10 ⁻³	100	1385	56.0	66.8
TEST B	6.8 10 ⁻³	106	1698	57.2	63.7
TEST C	7.3 10 ⁻³	122	1790	57.4	62.1
TEST D	7.8 10 ⁻³	135	1945	57.4	62.0
TEST E	8.3 10 ⁻³	149	2103	57.4	58.8
TEST F	8.8 10 ⁻³	168	2219	57.0	61.3
TEST G	9.3 10 ⁻³	202	2149	56.6	63.8
TEST H	9.8 10 ⁻³	231	2182	57.5	66.2
TEST I	10.3 10 ⁻³	244	2429	57.9	66.9
TEST J	10.8 10 ⁻³	254	2697	57.7	65.8
TEST K	11.3 10 ⁻³	266	2966	56.3	60.4

Tab.2 Test conditions summary and computed efficiencies

3. METHODOLOGY

3.1. VELOCITY PROFILE ESTIMATION

LDV measurements couldn't be achieved close to the hub of the micro-turbine due to the high level of reflection of the laser beam. Thus a method to fulfill the velocity profiles has been developed. A first hypothesis on the velocity profile shape has been done by taking the numerical simulations performed by Münch-Alligné *et al.* [2] as a reference. An interpolation by using third order Hermite polynomial has been done on the velocity profile of the meridional component by considering the measured average values.

$$C_m(r) = \sum_i b_i He_i(r) \quad (2)$$

The mass balance equation has been integrated on the profiles in order to compute the discharge \tilde{Q} in each investigated section.

$$\tilde{Q} = \int_A \vec{C} \cdot \vec{n} dA = \int_{R_h}^{R_s} 2\pi C_m(r) r dr \quad (3)$$

The discrepancies between the discharges computed in the three sections and the measured one has to be minimized. Thus an optimization problem has been solved whose objective function is defined by Eq.(4).

$$g(b_i) = \left| \int_{R_h}^{R_s} 2\pi C_m(r) r dr - Q \right| \quad (4)$$

$$\{b_i\} = \arg \min (g(b_i)) \quad (5)$$

The velocity values have been bounded within the standard deviation $\sigma(r)$ of the measured values as expressed in Eq.(6).

$$\bar{C}_m(r) - \sigma(r) \leq C_m(r) \leq \bar{C}_m(r) + \sigma(r) \quad (6)$$

A constrain on the first order derivatives has been imposed in order to respect the predicted shape of the velocity profile by the numerical simulation where measurements couldn't be reached. This optimization problem has been solved by using a genetic algorithm.

3.2. EFFICIENCY COMPUTATION

In order to compute the efficiency, the total specific rothalpy balance equation has been integrated on the profile to compute the transferred power by obeying Eq.(7):

$$\tilde{P}_t = \int_A \bar{\vec{C}} \cdot \vec{U} \rho \bar{\vec{C}} \cdot \vec{n} dA = 2\pi\rho\omega \left(\int_{R_h}^{R_s} C_{u1}(r) C_{m1}(r) r^2 dr + \int_{R_h}^{R_s} C_{u2}(r) C_{m2}(r) r^2 dr \right) \quad (7)$$

The efficiency has been computed according to Eq.(8):

$$\eta = \frac{E_t}{E_h} \quad (8)$$

where the transferred specific energy $E_t = \frac{P_t}{\rho Q}$ has been computed by solving the global Euler equation with the hypothesis of inviscid flow.

4. RESULTS

The measured flow velocity profiles at the investigated operational conditions of the counter rotating micro-turbine are presented in Fig.3 (meridional component) and Fig.4 (tangential component). The empty circles indicate the measured average values while the continuous lines are the results of the interpolation performed by optimizing the mass balance equation. All the values are normalized by the meridional absolute flow velocity with the hypothesis of having an uniform flow distribution, computed as follows in Eq.(9).

$$\tilde{C}_m = \frac{Q}{A} \quad (9)$$

The maximum difference between the measured discharges and the computed ones by integrating the mass balance equation is 3.1% of the measured discharge.

At the inlet section the measurements confirm a purely axial flow with a confident standard deviation along the span for both the meridional and tangential components. The velocity profiles of the meridional component cross the measured average values. This confirms the uniformity of the flow at the inlet section achieved by the honeycomb grid located upstream.

At the inter-runners section the turbulence level increases due to the influence of the blade passage of the two runners. The standard deviation reaches a maximum of 0.9 for the normalized measured meridional velocity. The flow is strongly affected by the wall effect at both the casing wall and the hub which is limiting the unrecovered energy. It is also strongly accelerated and deviated in the span causing the increase of the non-uniformities. This is confirmed by the results of the optimized interpolation of the velocity profile which is not crossing the measured average velocity values.

At the outlet section the flow the values of the meridional component which satisfy the mass balance equation are higher than the measured average velocity. It was impossible to reach these operational points with a significant counter pressure at the outlet due to the limited power provided by the pump on the test rig. Thus the counter-pressure has been decreased causing cavitation patterns on the blade of the second runner. The bubbles conducted downstream affected the measures of the velocity at the outlet causing an underestimation of the measured values. Moreover the un-recovered energy is limited by the casing wall effect.

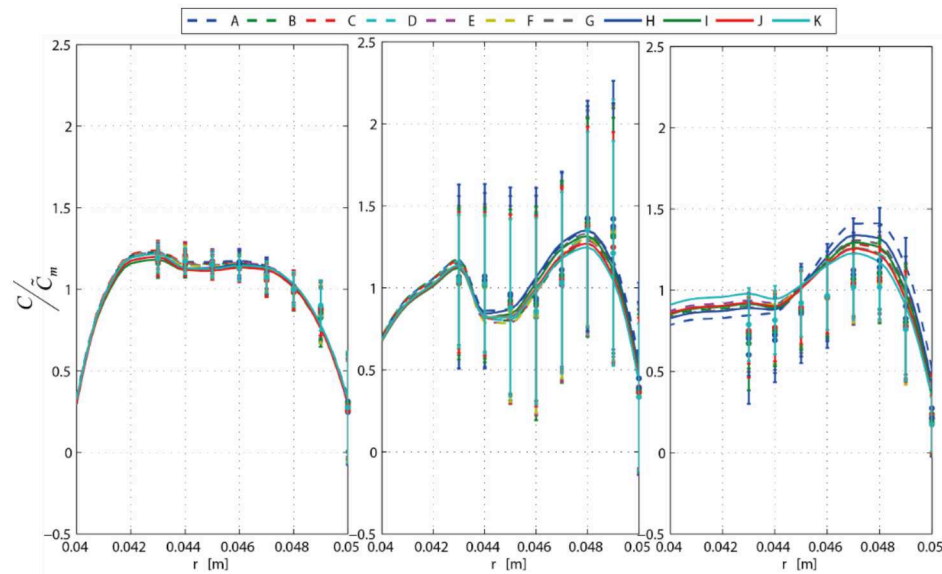


Fig.3 Meridional velocity profile at the inlet (left), inter-runners (center) and outlet (right).

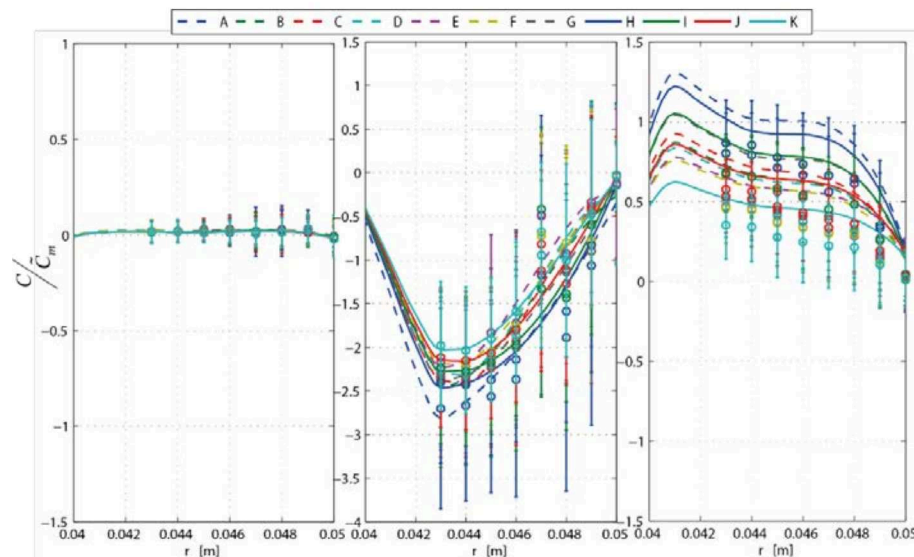


Fig.4 Tangential velocity profile at the inlet (left), inter-runners (center) and outlet (right).

The efficiencies computed by the integration of the total specific rothalpy balance equation are presented in Tab.2. Comparing with the efficiencies previously measured [3] the computed values are higher. This is due to the mechanical losses accounted for in the measurements presented by Andolfatto *et al.* [3] and which are not included in the efficiency computation by solving the total specific rothalpy balance equation and the Euler equation.

5. CONCLUSION

The flow velocity field along the meridional and tangential component has been investigated by performing LDV measurements in the counter rotating micro-turbine. A method to complete the flow velocity profile where LDV measurements were obstructed has been developed to find the optimal solution of the velocity values with respect to the mass balance equation in the three investigated sections. A method based on the resolution of the total specific rothalpy balance equation has been employed to compute the hydraulic power of the micro-turbine thus to compute the efficiency. These results achieved allow a better understanding on the performance of the counter rotating micro-turbine. They will address further improvements of the blade geometry and a better control of the machine regulations.

6. ACKNOWLEDGEMENTS

The research leading to the results published in this paper has received funding from SCCER SoE, the Swiss Energy Center for Energy Research Supply of Electricity granted by the Swiss Commission for Technology and Innovation (CTI); the Ark, the foundation for innovation of Valais Canton, through the Project HydroVS and from the Swiss Commission for Technology and Innovation as part of the DuoTurbo project number 17197.1 PFEN IW. The authors would like to thank the energy hydraulic team of the HES SO Valais for their collaboration and technical support.

REFERENCES

- [1] L. Andolfatto, C. Euzenat, E. Vagnoni, C. Munch-Alligné and F. Avellan, "A mixed standard/custom design strategy to minimize cost and maximize efficiency for Picohydro power potential harvesting," in *IYCE 2015, International Youth Conference on Energy 2015*, Pisa, Italy, 2015.
- [2] C. Münch-Alligné, S. Richard, B. Meier, V. Hasmatuchi and F. Avellan, "Numerical simulations of a counter-rotating micro-turbine," *SimHydro 2012, 12-14 September 2012, Sophia Antipolis*.
- [3] L. Andolfatto, J. Delgado, E. Vagnoni, C. Münch-Alligné and F. Avellan, "Analytical hillchart towards the maximization of energy recovery on water utility networks with counter rotating micro-turbine," *E-proceeding of the 36th IAHR World Congress 2015, The Hague, The Netherlands*.
- [4] E. Vagnoni, L. Andolfatto, J. Delgado, C. Münch-Alligné and F. Avellan, "Application of Laser Doppler Velocimetry to the development of a counter rotating micro-turbine," *E-proceeding of the 36th IAHR World Congress 2015, The Hague, The Netherlands*.
- [5] J. Gagnon, M. Iliescu, G. Ciocan and C. Deschênes, "Experimental Investigation of the runner outlet flow in axial turbine with LDV and stereoscopic PIV," in *IAHR 24th Symposium on Hydraulic Machinery and Systems*, Foz do Iguaçu, Brazil, 2008.
- [6] S. Zaidi, "Practical problems associated with laser anemometry in high speed turbomachines," *Optics and Laser in Engineering*, vol. 26, pp. 473-486, 1997.
- [7] A. Müller, M. Dreyer, N. Andreini and F. Avellan, "Draft tube fluctuations during self-sustained pressure surge: fluorescent particle image velocimetry in two-phase flow," *Experiments in Fluids*, vol. 54, no. 4, pp. 1-11, 2013.
- [8] O. Uzol, Y. Chow, J. Katz and C. Meneveau, "Unobstructed PIV measurements within an axial turbo-pump using liquid and blades with matched refractive index," *Experiments in Fluids*, vol. 33, pp. 909-919, 2002.
- [9] R. Miorini, H. Wu and J. Katz, "The internal structure of the tip leakage vortex within the rotor of an axial waterjet pump," *J. Turbomachines*, vol. 134, no. 3, 2011.

NOMENCLATURE

p	(Pa)	pressure	E	(J kg ⁻¹)	specific energy
\vec{C}	(m s ⁻¹)	absolute velocity	P	(W)	power
\vec{U}	(m s ⁻¹)	rotating velocity	η	(-)	efficiency
\vec{C}_m	(m s ⁻¹)	meridional velocity	\vec{C}_u	(m s ⁻¹)	tangential velocity
Q	(m ³ s ⁻¹)	discharge	ω	(rad s ⁻¹)	rotational speed
A	(m ²)	area	ρ	(kg m ⁻³)	density